

# **Efficient radiosynthesis of 3'-deoxy-3'-[<sup>18</sup>F]fluorothymidine using electrowetting-on-dielectric digital microfluidic chip**

Muhammad Rashed Javed<sup>1,2,3</sup>, Supin Chen<sup>4</sup>, Hee-Kwon Kim<sup>1,2,3</sup>, Liu Wei<sup>1,3,5</sup>, Johannes Czernin<sup>1,3,5</sup>, Chang-Jin "CJ" Kim<sup>4,6</sup>, R. Michael van Dam<sup>1,2,3,4</sup>, and Pei Yuin Keng<sup>1,2,3\*</sup>

<sup>1</sup>Department of Molecular and Medical Pharmacology, <sup>2</sup>Crump Institute for Molecular Imaging, <sup>3</sup>David Geffen School of Medicine, <sup>4</sup>Bioengineering Department, <sup>5</sup>Ahmanson Translation Imaging Division Mechanical, and <sup>6</sup>Aerospace Engineering Department  
University of California, Los Angeles, Los Angeles, CA 90095, U.S.A.

## **SUPPLEMENTAL INFORMATION**

### **EWOD chip fabrication**

The EWOD chip is constructed of two parallel plates: the base plate and the cover plate. The base plate has multitudes of thin-film electrodes designed for droplet routing, heating, and temperature sensing. The cover plate has a conductive layer to ground droplets for the EWOD actuation. Both plates were fabricated from 700 μm thick glass wafers coated with 140 nm of indium tin oxide (ITO) (Semiconductor Solutions LLC), onto which 20 nm of chrome and 200 nm of gold were deposited by electron-beam evaporation. Photolithography and wet etching of the metal layers were used to pattern EWOD electrodes, heaters, connection lines, and contact pads. A second photolithography step and wet etching removed gold and chrome from EWOD electrodes and heaters. A 2 μm layer and a 100 nm layer of silicon nitride was deposited onto the base plate and the cover plate, respectively, by plasma-enhanced chemical vapor deposition (PECVD) to serve as a dielectric. A 250 nm Teflon® layer was then spin-coated onto both plates and annealed at 330 °C to make the surfaces hydrophobic. The cover plate was bonded to the base plate using two layers of double-sided tape (3M Inc.) creating a 140 μm gap (measured with

a Vernier caliper).

### **EWOD Chip Operation**

EWOD actuation voltage for droplet movement was generated from a 10 kHz signal (33220A waveform generator, Agilent Technologies) amplified to 100 Vrms (Model 601C, Trek). The voltage was applied selectively to desired electrodes for droplet movement by individually addressable relays (AQW610EH PhotoMOS relay, Panasonic) that were controlled by a LabVIEW program using a digital I/O device (NI USB-6509, National Instruments). A second digital I/O device (NI USB-6259, national Instruments ) was used to control a multichannel heater driver that was designed and built in house to measure and maintain feedback-controlled temperatures over the chip's four individual heaters.(1) Each chip's multifunctional electrodes were individually connected to a switch to alternate between EWOD actuation voltage or temperature measurement and heating.

### **Quality control (QC) analysis of [<sup>18</sup>F]FLT**

#### *Gas chromatography for residual solvent analysis*

A quantitative method for determining amount of residual solvents in [<sup>18</sup>F]FLT was developed based on our previous report (1) using gas chromatography (Agilent 7890A) equipped with a mass spectroscopy detector, an auto sampler and a JW DB-WAX (polyethylene glycol) column (30 m long, 0.25 mm ID and a phase thickness of 0.25 μm). Supplemental Figure 2 shows a typical chromatogram of standard solutions of solvents and the representative chromatogram of the final [<sup>18</sup>F]FLT sample. The GC was operated in a helium flow of 1.5 mL/min. In this method, the initial oven temperature was set at 35°C and held for 2 min followed by a temperature ramp of 10°C/min to 80°C. After holding at 80°C for 0.5 minute, the temperature was ramped at

10°C/min to 150°C and held for 10 minutes to separate the mixtures.

#### *Chemical and radiochemical purity analysis*

The radiochemical purity of final [ $^{18}\text{F}$ ]FLT was determined by the radioactive thin layer chromatography (radio-TLC) and radioactive HPLC. A small aliquot of the formulated product was spotted onto a silica gel plate and was developed with 50:50 (vol/vol) ethyl acetate/ethanol. After the silica gel plate was developed in the solvent mixture, the radioactivity distribution was scanned using the radio-TLC scanner (MiniGITA star). Using this TLC solvent system, the unreacted fluoride remained on the baseline with  $R_f$  of 0, while the [ $^{18}\text{F}$ ]FLT appeared at  $R_f$  of 0.84. Upon the cartridge purification, the radio-TLC of the purified [ $^{18}\text{F}$ ]FLT TLC showed only one peak at  $R_f$  of 0.84, confirming that the unreacted fluoride was effectively removed during the cartridge purification process to yield > 99% radiochemical purity.

The chemical purity of the final [ $^{18}\text{F}$ ]FLT sample was analyzed on the radio-HPLC equipped with the Phenomenex Luna reversed-phase C-18 column (250 x 4.6 mm), with isocratic elution of  $\text{H}_2\text{O}$ /ethanol 90:10 (v/v) at a flow rate of 1 mL/min. Calibration curve of standard solution of FLT and other common impurities found in the synthesis of [ $^{18}\text{F}$ ]FLT were performed on the same analytical HPLC using a UV detection at 265 nm. The isocratic analytical radio-HPLC chromatogram showed the production of [ $^{18}\text{F}$ ]FLT with several chemical impurities detected in UV chromatogram. During the process optimization, the extent of hydrolysis was analyzed using the analytical HPLC under the same condition. The fully hydrolyzed [ $^{18}\text{F}$ ]FLT contained only a single radio-peak which elutes at ~ 15 minutes in the radio-HPLC. Under an unoptimized hydrolysis condition, a small (5%) of radio-peak emerged at around 16 minutes, which is presumably the partially hydrolyzed [ $^{18}\text{F}$ ]FLT.

#### **EWOD chip for radiosynthesis**

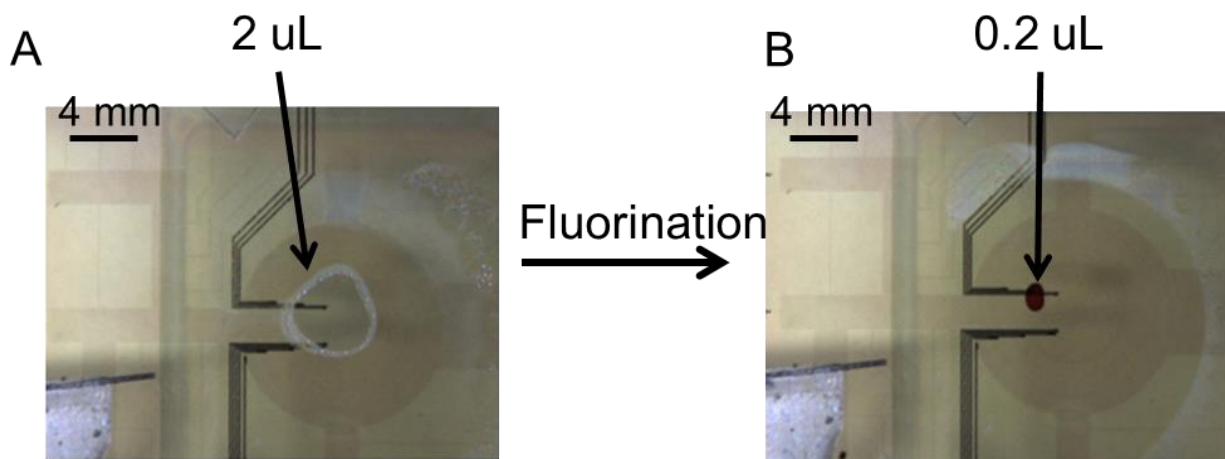
Droplets sandwiched between the plates of the EWOD chip are moved by electrowetting when an electrical potential is applied to electrodes on the base plate to accomplish operations such as droplet generation, transport, splitting and mixing.(2) The EWOD electrodes at the reaction site are capable of resistive heating and thermistic temperature sensing in addition to droplet movement (Supplemental Figure 1(b)).(3) The reaction site electrodes were configured as four concentric rings (12 mm diameter) to center droplets and accurately control their temperature as they shrink. Each of the four rings is independently capable of feedback temperature control, an important feature for maintaining a desired reaction site temperature, as the droplet size shrinks due to evaporation resulted in dry regions of the heater, which require less power than heater region that are still wetted with a liquid droplet.

### **Animal Experiments**

The human epidermis carcinoma cell line A431 was purchased from American Type Culture Collection (ATCC). Cells were cultured in Dulbecco's modified Eagle medium supplemented with 10% fetal bovine serum (Invitrogen, United States) at 37°C in 5% CO<sub>2</sub>. Severe combined immune deficient (Scid/Scid) mice were purchased from The Jackson Laboratory (Sacramento, CA). All animal manipulations were conducted with sterile techniques following the guidelines of the University of California at Los Angeles Animal Research Committee. To generate tumor model, A431 cells that growing exponentially in culture were suspended in PBS and Matrigel (BD Biosciences, Franklin Lakes, NJ) and injected subcutaneously at the right shoulder of the animal. After tumor had grown to an approximate size, mice were used for the PET/CT imaging study.

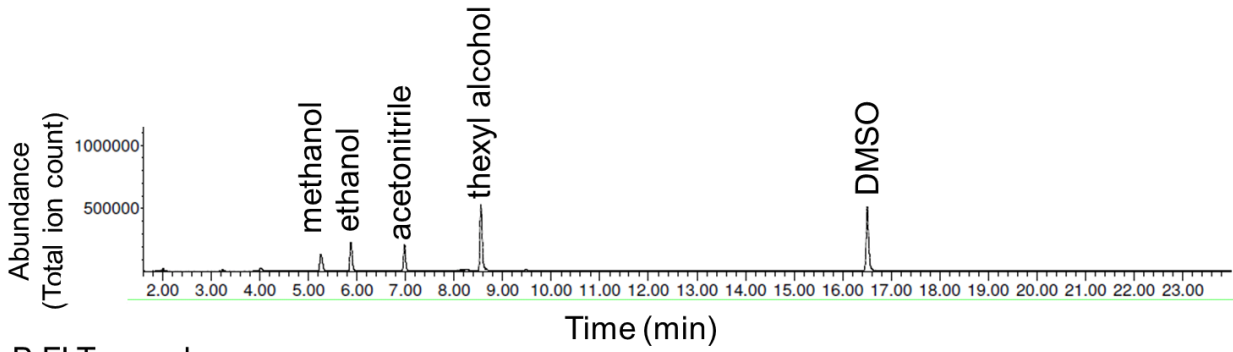
### **MicroPET and CT imaging**

MicroPET/CT scans were performed using the microPET Inveon scanner (Siemens Preclinical Solutions, Malvern, PA) and MicroCATII CT scanner (Siemens Preclinical Solutions, Malvern, PA). The mice were injected in the tail vein with 1.5 to 1.7 MBq of [ $^{18}\text{F}$ ]FLT in saline under conscious condition. After 60 minutes of uptake time, the mice were anesthetized with 2% isoflurane and were placed in the microPET and microCT chambers. All image analysis was performed using the OsiriX (Pixmeo, Geneva, Switzerland) software. The biodistribution of the [ $^{18}\text{F}$ ]FLT in the xenografted mice showed high uptake in the tumor as expected (Supplemental Fig. 7).

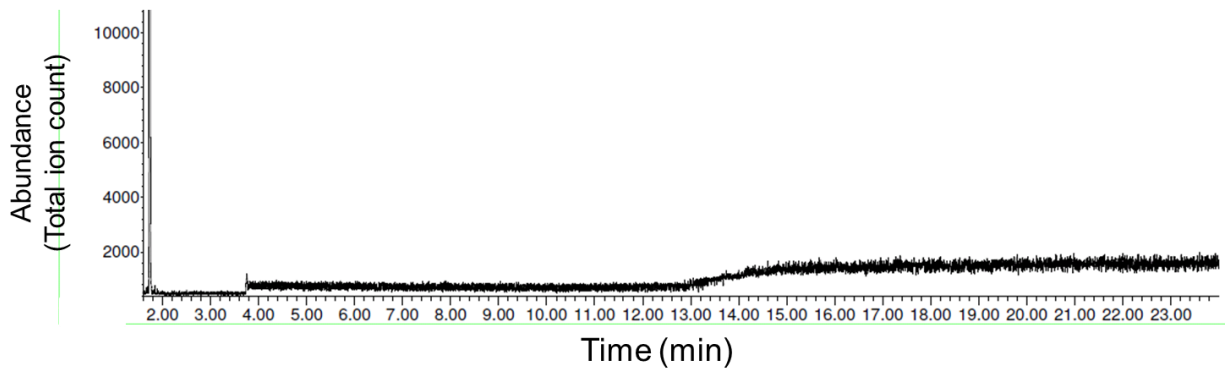


Supplemental Fig. 1: Representative images of the reaction droplet (A) before the fluorination reaction and (B) at the end of the fluorination reaction. The droplet size shrunk from 2  $\mu\text{L}$  to 0.2  $\mu\text{L}$  at the end of the fluorination reaction.

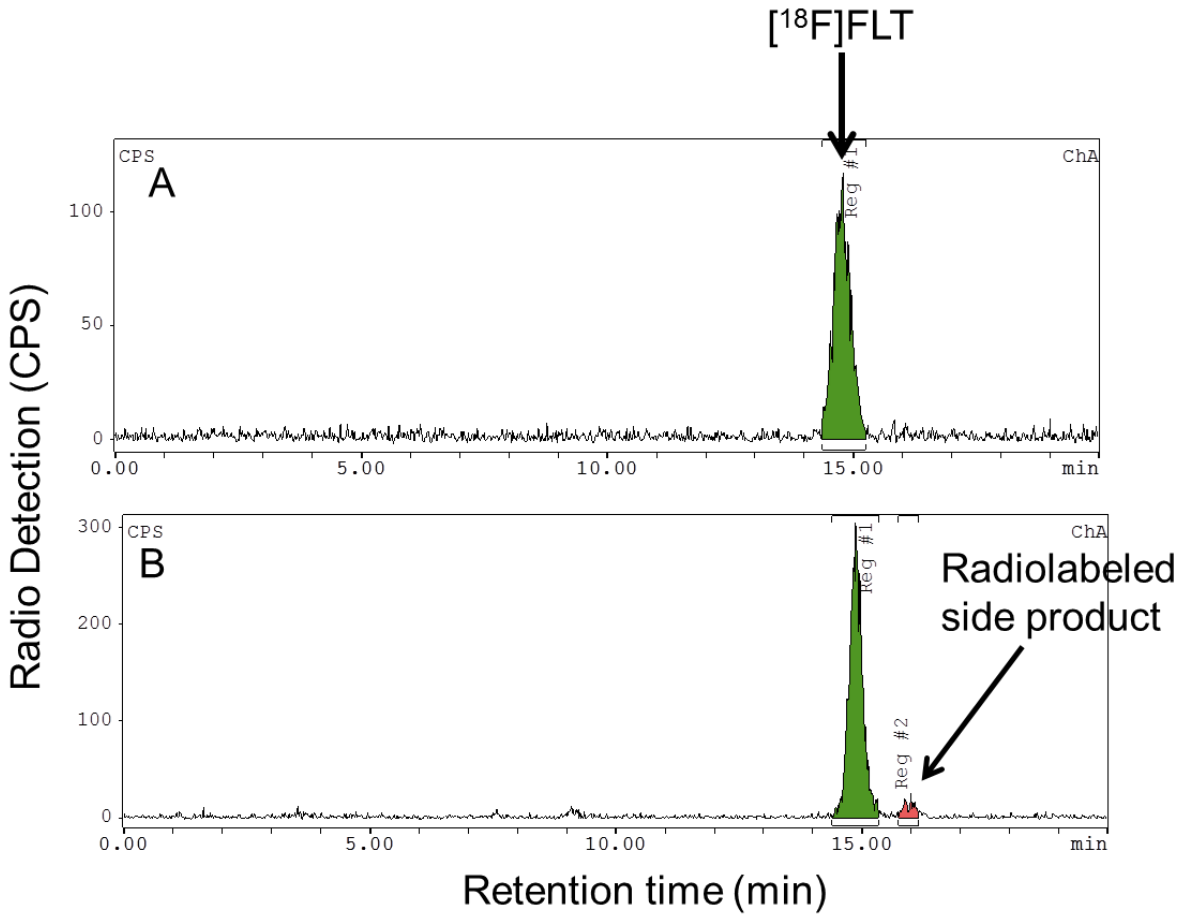
A Standard mixtures



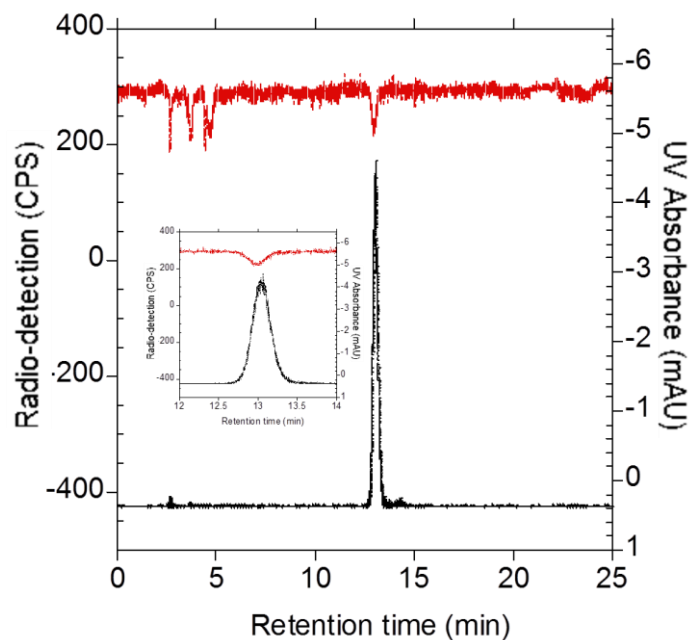
B FLT sample



Supplemental Fig. 2: A representative GC chromatogram of the (A) standard solvent mixtures and (B) the final [<sup>18</sup>F]FLT sample.

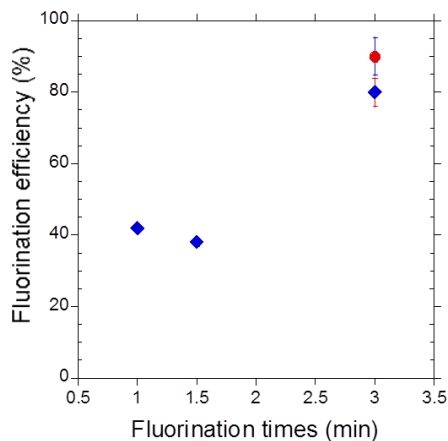


Supplemental Fig. 3: Radio-HPLC of crude  $[^{18}\text{F}]\text{FLT}$  mixtures. Representative chromatogram of (A) a fully hydrolyzed  $[^{18}\text{F}]\text{FLT}$ , and (B) partially hydrolyzed  $[^{18}\text{F}]\text{FLT}$ .

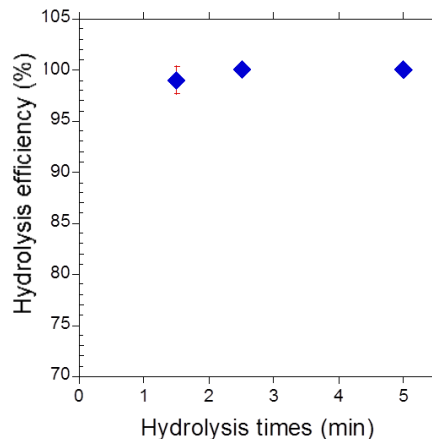


Supplemental Fig. 4: HPLC chromatogram used for specific activity analysis of [ $^{18}\text{F}$ ]FLT. The inset showed a narrow region where both the UV and radio peaks of FLT can be observed and quantitate.

A Kinetics of fluorination and fluorination efficiency

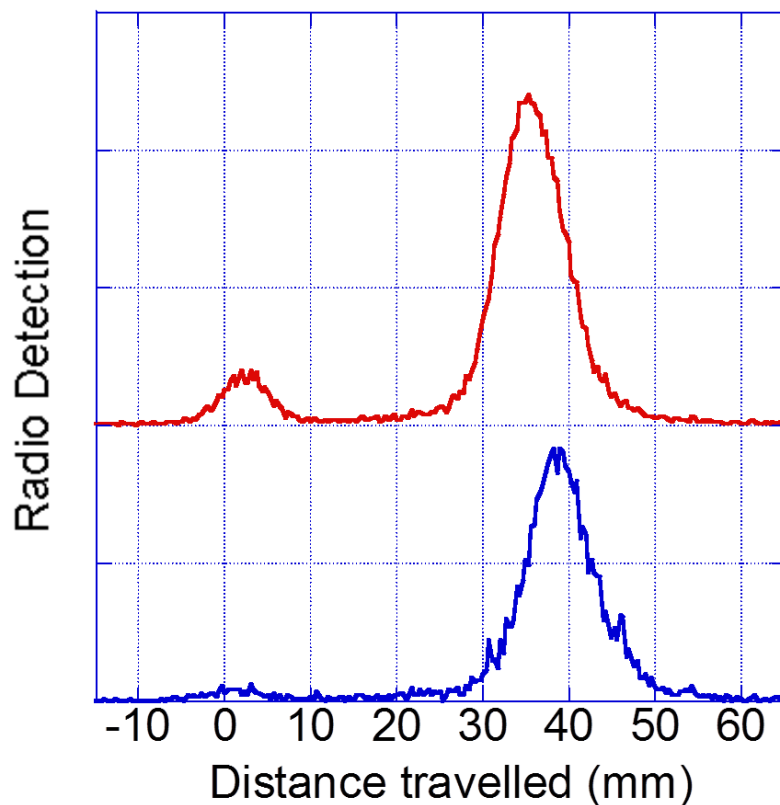


B Kinetics of hydrolysis reaction

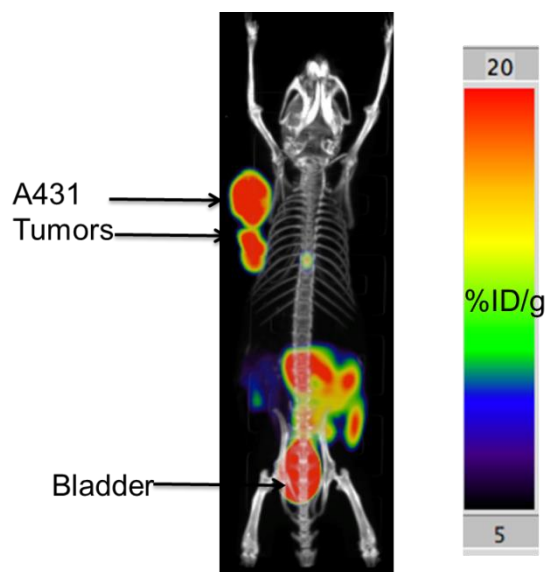


Supplemental Fig. 5: The effect of reaction time in the (A) fluorination and (B) hydrolysis efficiencies. The concentration of the precursor and phase transfer catalyst is 90 mM and 45 mM, respectively. The fluorination reaction was performed in a 2  $\mu\text{L}$  droplet mixture of the xyl alcohol and DMSO in 1:2 (v/v) ratios at 120  $^{\circ}\text{C}$ . The hydrolysis reaction was performed in 7  $\mu\text{L}$  mixture of 1N HCl and MeCN in 4:1 v/v ratios at 95  $^{\circ}\text{C}$ .





Supplemental Fig. 6: Representative radio-TLC chromatogram of the crude [ $^{18}\text{F}$ ]FLT mixture (red trace) and the cartridge purified [ $^{18}\text{F}$ ]FLT (blue trace). The unreacted [ $^{18}\text{F}$ ]fluoride ion with  $R_f$  of 0 was successfully removed upon the cartridge purification as shown in the blue chromatogram.



Supplemental Fig. 7: Biodistribution of [ $^{18}\text{F}$ ]FLT, synthesized on EWOD chip, in a mouse bearing A431 tumors.

## REFERENCES

1. Keng PY, Chen S, Sadeghi S, et al. Digital microfluidics for multi-step batch chemical synthesis: Application to synthesis of radiotracers for positron emission tomography (pet). *Proc. Natl. Acad. Sci. U.S.A.* 2012;109(3):690-695.
2. Cho SK, Moon H, Kim C-J. Creating, transporting, cutting, and merging liquid droplets by electrowetting-based actuation for digital microfluidic circuits. *Microelectromechanical Systems, Journal of.* 2003;12(1):70-80.
3. Nelson WC, Peng I, Lee G-A, Loo JA, Garrell RL, “Cj” Kim C-J. Incubated protein reduction and digestion on an electrowetting-on-dielectric digital microfluidic chip for maldi-ms. *Anal Chem.* 2010;82(23):9932-9937.